Cross-Image Context for Single Image Inpainting – Supplementary Material –

Tingliang Feng, Wei Feng, Weiqi Li, Di Lin*
College of Intelligence and Computing, Tianjin University
{fengtl, wicky}@tju.edu.cn, wfeng@ieee.org, Ande.lin1988@gmail.com

1 Implementation Details

We use the PyTorch toolkit to implement our inpainting network with CICM. The network is optimized by the Adam solver for 400,000 iterations. The initial learning rate is 0.0001, which is linearly decayed during the network training. Each mini-batch contains 8 images with the size of 256×256. We randomly crop and flip the training images to augment the data. The network is trained on 4 RTX 2080Ti GPUs.

In our implementation, we use a warm-up strategy to pre-train the backbone network for 50,000 iterations. The encoder of the pre-trained backbone is used to compute the regional features of different images. We conduct k-means clustering on the regional features, computing the cluster centers as the initial anchor features. The regional features, which are nearest to the initial anchor features, are selected as the initial cross-image features in different sets of CICM.

To augment the training data, we generate the corrupted regions in the training images, by randomly matching the irregular masks [1, 2, 3] and the RGB images. For a fair comparison during the network testing, the corrupted regions in the testing images are fixed for different methods.

2 Supplementary Experiments

In this section, we provide more details of the experiments. We divide this section into four parts. The first part is a supplementary description of experimental setups in the main paper. The second part is the convergence analysis of our network training. The third part is the analysis on distributions of cross-image features. The fourth part is to show more visual results on different datasets.

2.1 Supplementary Description of Experimental Setup

Variants of Context Generalization In Table 1 ("Context Generalization"), which has been presented in the main paper, we use different ways of updating the cross-image features for context generalization. Given a regional feature, we find the most relevant feature set, where all of the cross-image features are updated (see "100% update"). We experiment with reducing the number of cross-image features to be updated. This is done by ranking the similarities between the regional feature and cross-image features, and selecting the top-50% (or even top-1) cross-image features for updating.

After calculating the similarities between the regional feature $\mathbf{F}_n$ and the cross-image features in the chosen feature set, we need to update the cross-image features for context generalization. Here, we use three different ways of updating, as illustrated in Figure 1. In Figure 1(a), we only update the cross-image feature that has the highest similarity with the regional feature $\mathbf{F}_n$. In Figure 1(b), we update the top-50% cross-image features according to the similarities. In Figure 1(c), we update all the cross-image features in the chosen feature set.

*Di Lin is the corresponding author of this paper.

36th Conference on Neural Information Processing Systems (NeurIPS 2022).

Context Generalization															
Methods	PSNR ↑			SSIM ↑			L1 ↓			LPIPS ↓			FID ↓		
	0-20%	20-40%	40-60%	0-20%	20-40%	40-60%	0-20%	20-40%	40-60%	0-20%	20-40%	40-60%	0-20%	20-40%	40-60%
w/o intra	28.032	20.711	16.647	0.9014	0.7566	0.5790	1.375	5.065	8.280	0.1277	0.2401	0.4369	22.75	53.75	129.3
w/o inter	27.954	20.384	16.338	0.8979	0.7521	0.5761	1.422	5.347	8.744	0.1243	0.2419	0.4423	24.36	55.73	132.7
intra & inter	**29.214**	**21.728**	**19.211**	**0.9205**	**0.8047**	**0.6258**	**1.079**	**3.478**	**6.375**	**0.0829**	**0.2045**	**0.3284**	**17.21**	**45.17**	**78.49**
top-1 update	28.021	20.309	16.632	0.9047	0.7692	0.5893	1.316	4.366	7.895	0.1186	0.2386	0.3918	21.86	59.73	126.4
top-50% update	28.413	20.923	17.118	0.9073	0.7731	0.5924	1.238	3.826	7.094	0.1017	0.2227	0.3642	20.57	56.39	106.4
100% update	**29.214**	**21.728**	**19.211**	**0.9205**	**0.8047**	**0.6258**	**1.079**	**3.478**	**6.375**	**0.0829**	**0.2045**	**0.3284**	**17.21**	**45.17**	**78.49**

Context Augmentation															
Methods	PSNR ↑			SSIM ↑			L1 ↓			LPIPS ↓			FID ↓		
	0-20%	20-40%	40-60%	0-20%	20-40%	40-60%	0-20%	20-40%	40-60%	0-20%	20-40%	40-60%	0-20%	20-40%	40-60%
w/o ratio	28.551	21.217	18.879	0.9112	0.7983	0.6219	1.211	3.502	6.423	0.0891	0.2102	0.3310	19.02	55.21	85.48
w/ ratio	29.214	21.728	19.211	0.9205	0.8047	0.6258	1.079	3.478	6.375	0.0829	0.2057	0.3284	17.21	45.17	78.49
w/ GT	**29.241**	**21.801**	**19.262**	**0.9227**	**0.8074**	**0.6281**	**1.074**	**3.462**	**6.356**	**0.0821**	**0.2040**	**0.3269**	**16.35**	**40.22**	**73.31**
top-1 aug	28.317	19.878	17.866	0.9092	0.7882	0.6031	1.164	3.624	7.173	0.0921	0.2179	0.3531	20.81	72.78	95.64
top-50% aug	28.800	20.828	18.295	0.9152	0.7962	0.6115	1.122	3.576	6.724	0.0875	0.2115	0.3376	18.83	63.32	87.35
100% aug	**29.214**	**21.728**	**19.211**	**0.9205**	**0.8047**	**0.6258**	**1.079**	**3.478**	**6.375**	**0.0829**	**0.2045**	**0.3284**	**17.21**	**45.17**	**78.49**

Table 1: The results of various generalization and augmentation ways on the test set of Places2.

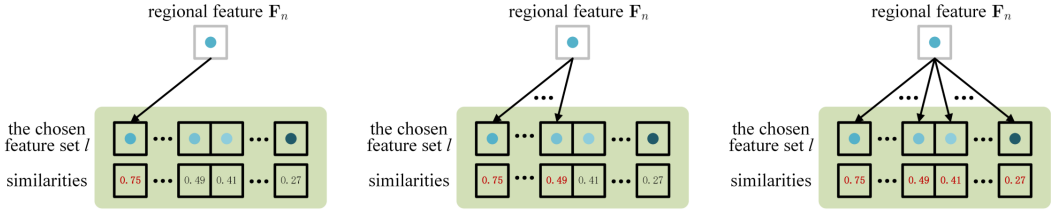

(a) top-1 update (b) top-50% update (c) 100% update

Figure 1: Three different ways of updating the cross-image features in the chosen feature set according to the similarities with the regional feature $\mathbf{F}_n$. (a) Updating the cross-image feature with the highest similarity. (b) Updating the top-50% cross-image features. (c) Updating all the cross-image features.

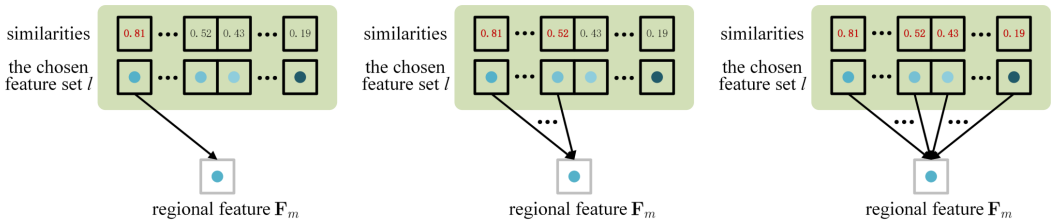

(a) top-1 augmentation (b) top-50% augmentation (c) 100% augmentation

Figure 2: Three different ways of the regional feature $\mathbf{F}_m$ augmentation according to the similarities with the cross-image features in the chosen feature set. (a) Augmentation by using the cross-image feature with the highest similarity. (b) Augmentation by using the top-50% cross-image features. (c) Augmentation by using all cross-image features.

Variants of Context Augmentation In Table 1 ("Context Augmentation"), which has been presented in the main paper, we study the impact of changing the number of the cross-image features, which are used by the context augmentation of the regional features. Note that our full model resorts to all of the cross-image features in the relevant set for feature augmentation (see "100% aug"). Based on the similarities between the cross-image features and the regional features, we select the top-1 and top-50% of the cross-image features, respectively, for augmenting the regional features. We illustrate these variants of context augmentation in Figure 2.

In Figure 2(a), we only choose the cross-image feature with the highest similarity to augment the regional feature $\mathbf{F}_m$. In Figure 2(b), we use the top-50% cross-image features according to the similarities for augmentation. In Figure 2(c), the whole cross-image features in the chosen feature set are used for context augmentation.

Different Ways of Using Image Context In Table 2 ("Single-Image Context"), which has been presented in the main paper, we report the results of using k-means and the deep-learning-based

Single-Image Context															
Methods	PSNR ↑			SSIM ↑			L1 ↓			LPIPS ↓			FID ↓		
	0-20%	20-40%	40-60%	0-20%	20-40%	40-60%	0-20%	20-40%	40-60%	0-20%	20-40%	40-60%	0-20%	20-40%	40-60%
k-means	28.311	20.946	17.021	0.9092	0.7734	0.5882	1.217	4.275	7.302	0.1049	0.2369	0.3992	20.21	61.37	110.4
RUC	28.386	20.997	17.105	0.9104	0.7763	0.5921	1.194	4.113	7.189	0.1025	0.2346	0.3927	19.46	67.71	106.6
anchor only	28.417	21.015	17.235	0.9120	0.7828	0.5977	1.164	3.872	7.071	0.0998	0.2320	0.3875	18.67	56.52	102.5
Cross-Image Context															
Methods	PSNR ↑			SSIM ↑			L1 ↓			LPIPS ↓			FID ↓		
	0-20%	20-40%	40-60%	0-20%	20-40%	40-60%	0-20%	20-40%	40-60%	0-20%	20-40%	40-60%	0-20%	20-40%	40-60%
merged sets	28.833	21.054	17.574	0.9130	0.7883	0.6035	1.145	3.721	6.857	0.0882	0.2217	0.3638	19.23	53.44	96.47
CICM	**29.214**	**21.728**	**19.211**	**0.9205**	**0.8047**	**0.6258**	**1.079**	**3.478**	**6.375**	**0.0829**	**0.2045**	**0.3284**	**17.21**	**45.17**	**78.49**

Table 2: The results of various ways of using context information on the test set of Places2.

RUC [4], which are the clustering methods for harnessing the single-image context in our scenario. In Figure 3, we show the process of using the clustering methods. For a single image, we use the clustering methods to divide the regional features of the complete regions into several clusters. Based on the similarities with the cluster centers, we find the most relevant regional features for augmenting the regional features of the corrupted regions. In the scenario of using the single-image context, we release the memory that stores different clusters of the regional features of each image, after using each mini-batch to optimize the network parameters.

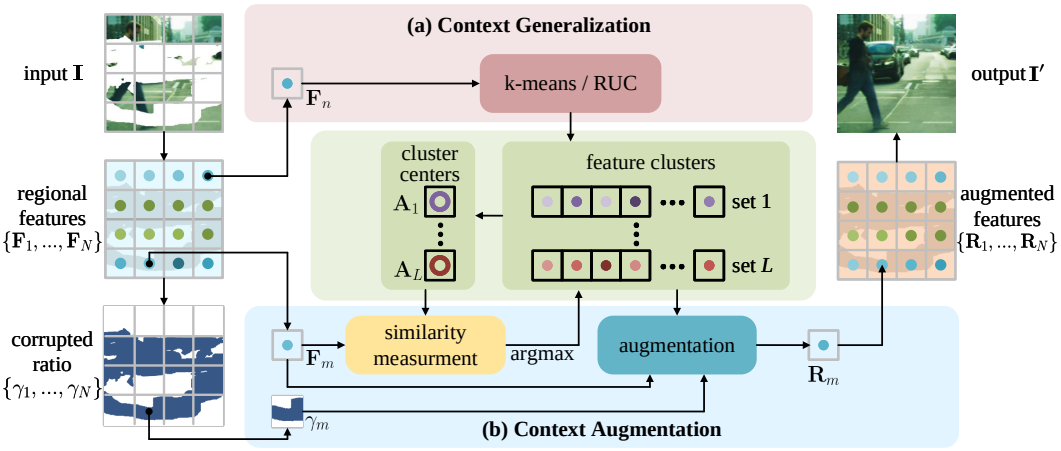

Figure 3: (a) For the regional features of the complete regions, the context generalization uses the clustering method (k-means or RUC) to cluster the regional features, where each cluster has a center. (b) Given a regional feature of the corrupted region, the context augmentation measures the similarity with every cluster center. It selects the cluster, where all regional features are used to augment the regional feature of the corrupted region.

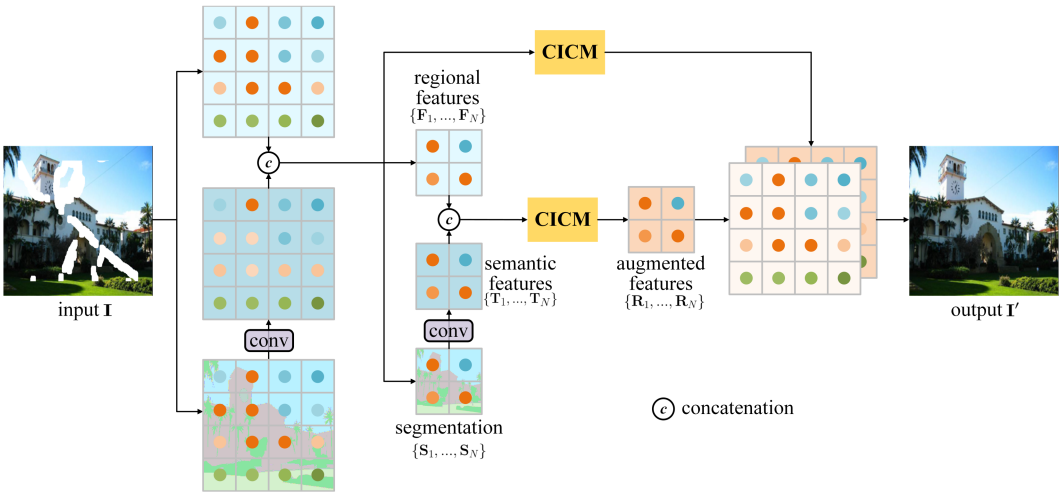

Figure 4: The extensive counterpart of our inpainting network with CICM. The network contains a lightweight segmentation sub-network for computing the semantic features.

Extensive Evaluation on Semantic Inpainting We extensively evaluate CICM on the public datasets (i.e., Cityscapes and Outdoor Scenes), which provide the semantic object categories for assisting the image inpainting task. Here, CICM can be easily extended to learn the cross-image features from not only the RGB images but also the semantic segmentation results. The results have been presented in Table 3 (also see Table 5 of the main paper).

In Figure 4, we provide more details of extending CICM. Along with the inpainting network, we train a lightweight semantic segmentation sub-network, which outputs the segmentation scores for all pixels in the input image. The segmentation scores are fed to a convolutional layer, which computes the semantic features. We concatenate the semantic features with the regional features. The concatenated features are used for computing the cross-image features in CICM.

Cityscapes Dataset															
Methods	PSNR ↑			SSIM ↑			L1 ↓			LPIPS ↓			FID ↓		
	0-20%	20-40%	40-60%	0-20%	20-40%	40-60%	0-20%	20-40%	40-60%	0-20%	20-40%	40-60%	0-20%	20-40%	40-60%
Gated [2]	35.870	27.011	22.938	0.965	0.801	0.748	0.518	2.627	3.872	0.0345	0.0576	0.1573	5.298	23.28	52.29
PEN [5]	33.693	23.927	22.336	0.964	0.800	0.694	0.548	3.132	4.012	0.0317	0.0552	0.1662	8.314	48.67	66.70
SPG [6]	29.627	25.425	21.863	0.900	0.817	0.718	0.722	2.877	4.188	0.0412	0.0610	0.1627	17.14	27.09	36.42
SWAP [7]	32.973	26.112	22.984	0.965	0.885	0.782	0.602	2.435	3.762	0.0365	0.0547	0.1543	6.327	15.48	29.32
SPL [8]	35.543	27.639	23.530	0.969	0.892	0.773	0.476	2.192	3.353	0.0311	0.0486	0.1263	4.686	12.94	28.81
CICM	**36.728**	**29.848**	**25.625**	**0.978**	**0.912**	**0.844**	**0.421**	**1.748**	**2.943**	**0.0281**	**0.0465**	**0.1170**	**3.437**	**8.246**	**12.16**
Outdoor Scenes Dataset															
Methods	PSNR ↑			SSIM ↑			L1 ↓			LPIPS ↓			FID ↓		
	0-20%	20-40%	40-60%	0-20%	20-40%	40-60%	0-20%	20-40%	40-60%	0-20%	20-40%	40-60%	0-20%	20-40%	40-60%
Gated [2]	30.826	24.262	19.294	0.955	0.874	0.680	0.910	2.018	2.684	0.0778	0.1578	0.2320	20.23	49.42	89.84
PEN [5]	29.072	21.515	19.237	0.949	0.796	0.630	1.036	2.438	2.711	0.0781	0.1662	0.2533	19.82	59.78	90.21
SPG [6]	24.156	21.692	18.282	0.801	0.685	0.533	1.417	2.638	2.764	0.0865	0.2218	0.2764	46.48	72.96	101.3
SWAP [7]	30.361	25.116	20.832	0.948	0.861	0.702	0.832	1.866	2.495	0.0572	0.1683	0.2217	13.29	40.01	63.86
SPL [8]	32.599	25.485	21.083	0.961	0.864	0.710	0.749	1.729	2.387	0.0465	0.1304	0.2042	11.24	30.07	53.28
CICM	**33.271**	**26.467**	**22.116**	**0.969**	**0.886**	**0.732**	**0.674**	**1.411**	**2.011**	**0.0412**	**0.1141**	**0.1872**	**8.684**	**23.35**	**42.47**

Table 3: Comparison with state-of-the-art methods on the test sets of Cityscapes and Outdoor Scenes.

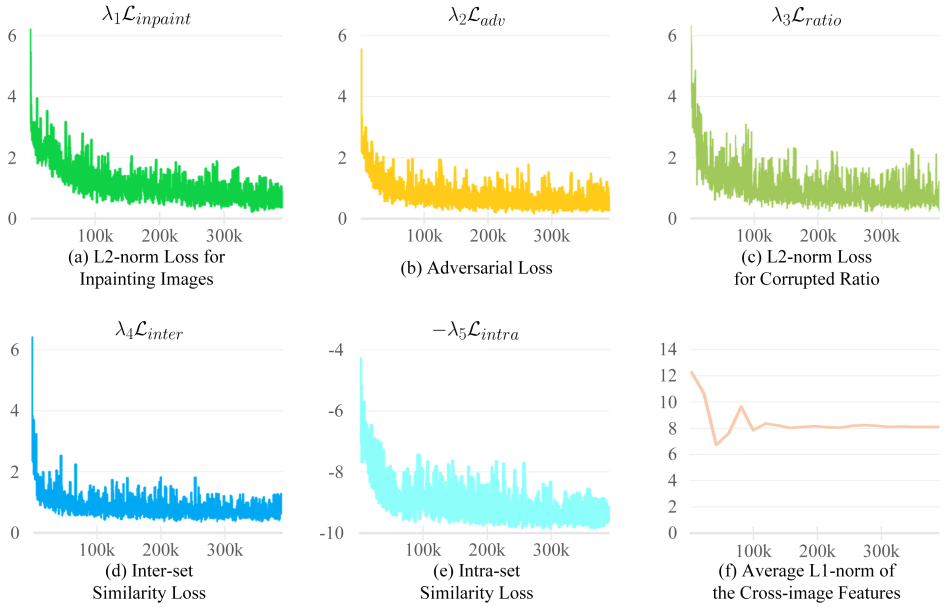

(a) L2-norm Loss for Inpainting Images (b) Adversarial Loss (c) L2-norm Loss for Corrupted Ratio

(d) Inter-set Similarity Loss (e) Intra-set Similarity Loss (f) Average L1-norm of the Cross-image Features

Figure 5: Analysis of convergence of the network training.

2.2 Analysis on Convergence of Network Training

To analyze the convergence of the network training, we show the changes of L2-norm and adversarial loss for penalizing the inpainting error, L2-norm for penalizing the estimation error of the corrupted ratios, inter-set and negative intra-set similarities, and average L1-norm of the cross-image features in CICM. The results are reported in Figure 5 (a–f), where the changes converge stalely at the final stages of the network training.

2.3 Analysis on Distributions of Cross-Image Features

We show the distributions of the cross-image features in CICM on different datasets in Figure 6. Here, we resort to t-SNE [9] for the visualization of the distributions of the cross-image features in the 2D space. During the network training, we also compute the weighted average of the image regions, whose regional features are injected by the context generalization into the cross-image features. We also show the average image regions in the corners of Figure 6. We find that most of the cross-image features, which belong to the same set, appear close to each other and represent similar visual patterns.

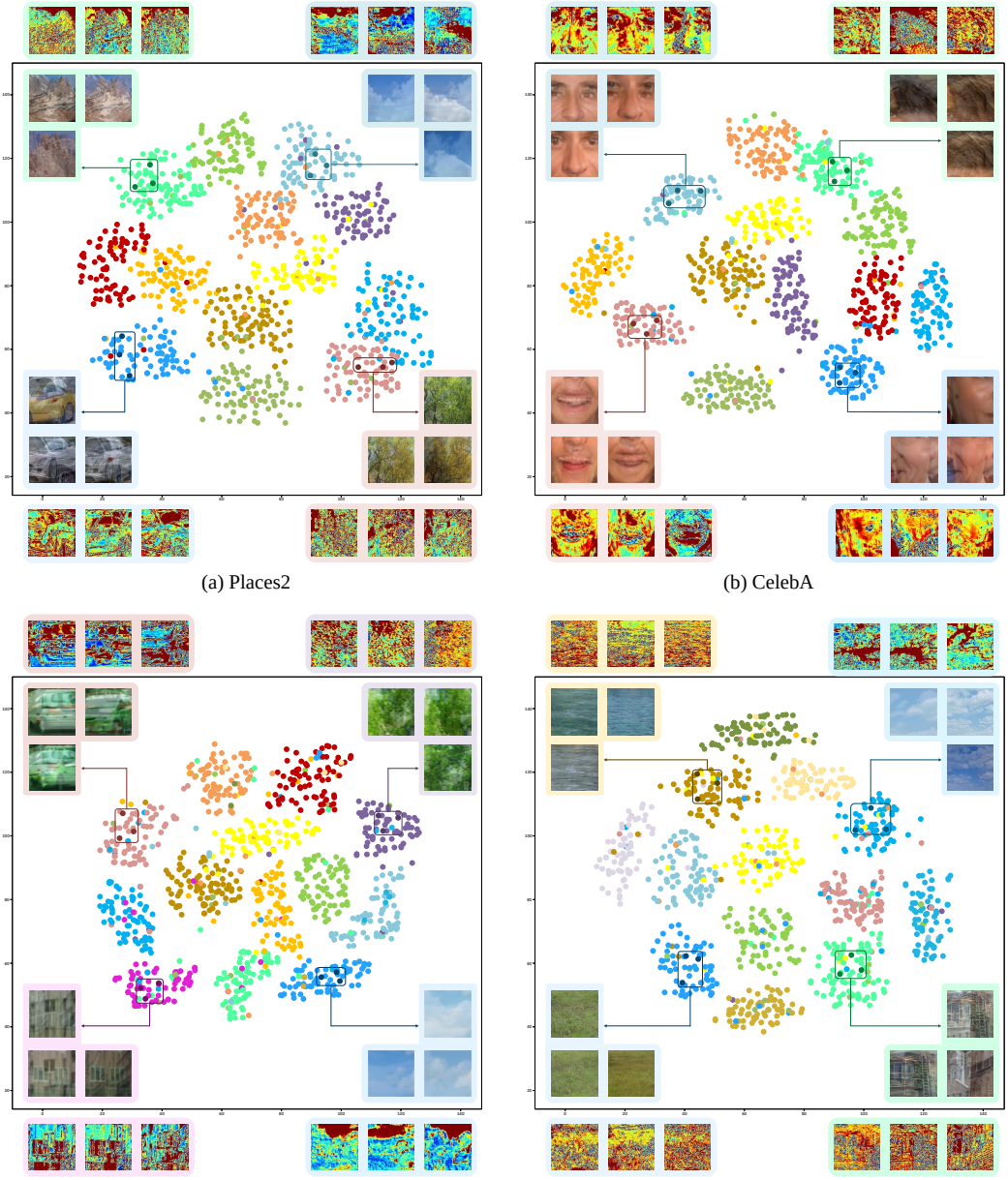

(a) Places2 (b) CelebA

(c) Cityscapes (d) Outdoor Scenes

Figure 6: Distribution of the cross-image features in CICM on different datasets. A scatter point represents a cross-image feature, which is embedded into the 2D space. The scatter points with the same color represent the cross-image features in the same set of CICM.

2.4 More Visual Results

We provide more visual results on Places2, CelebA, Cityscapes and Outdoor Scenes in Figures 7, 8, 9, and 10. As shown in these visual results, our inpainting network with CICM generally produces the high-quality results.

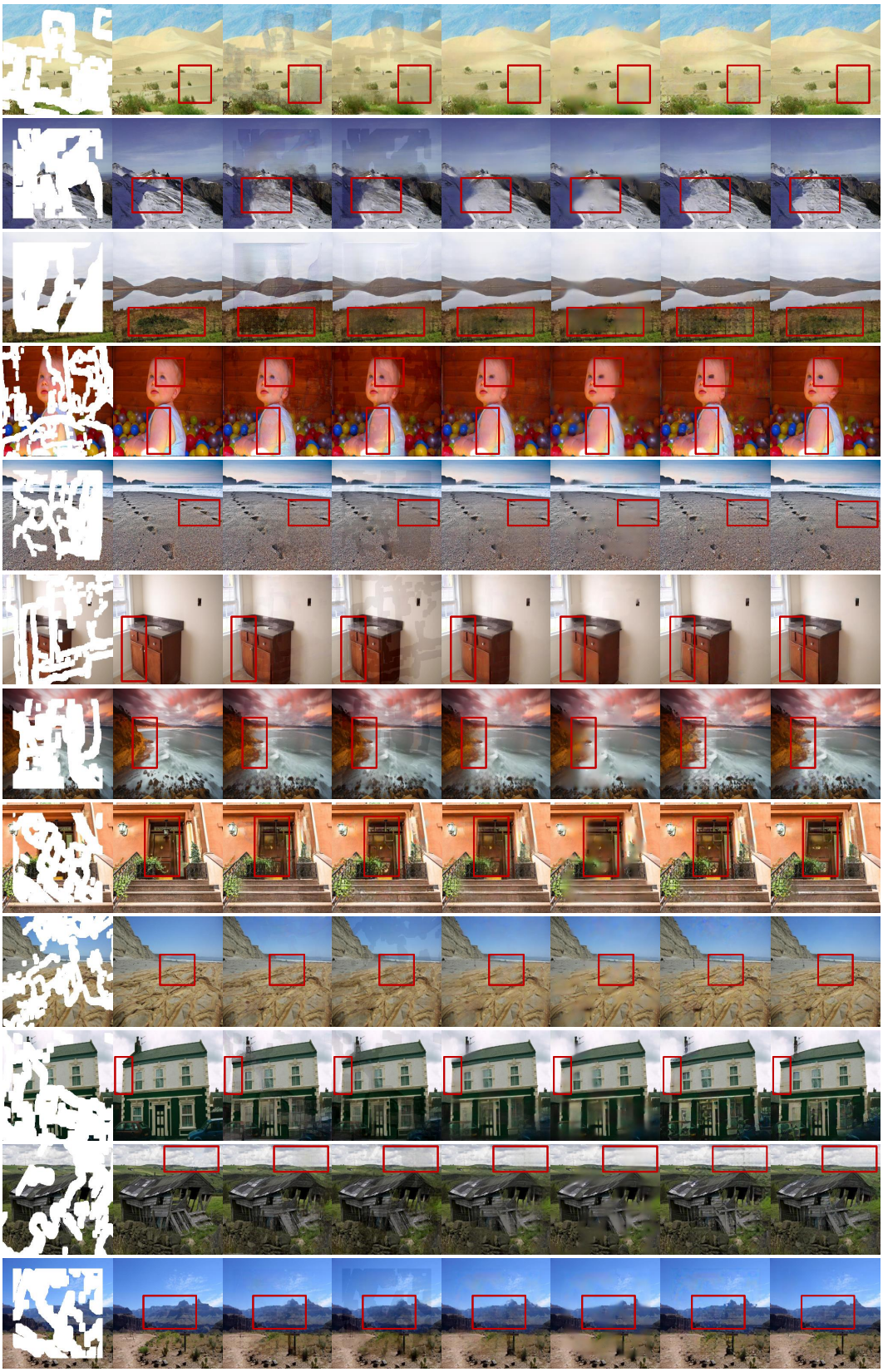

Figure 7: Visual results of RFR [10], JPG [11], MISF [12], TMAD [13], SRM [14] and CICM on the test set of Places2.

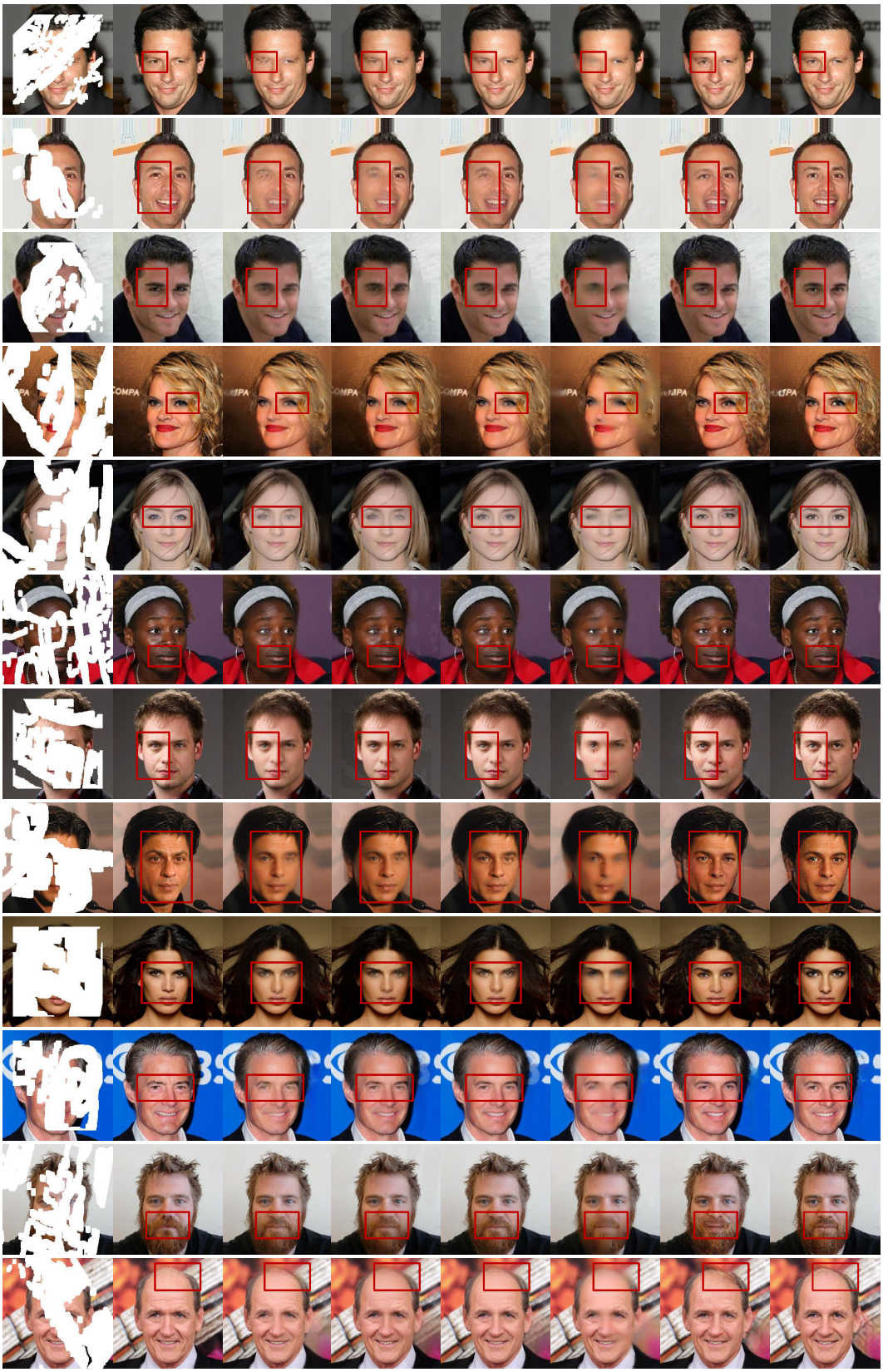

Figure 8: Visual results of RFR [10], JPG [11], MISF [12], TMAD [13], SRM [14] and CICM on the test set of CelebA.

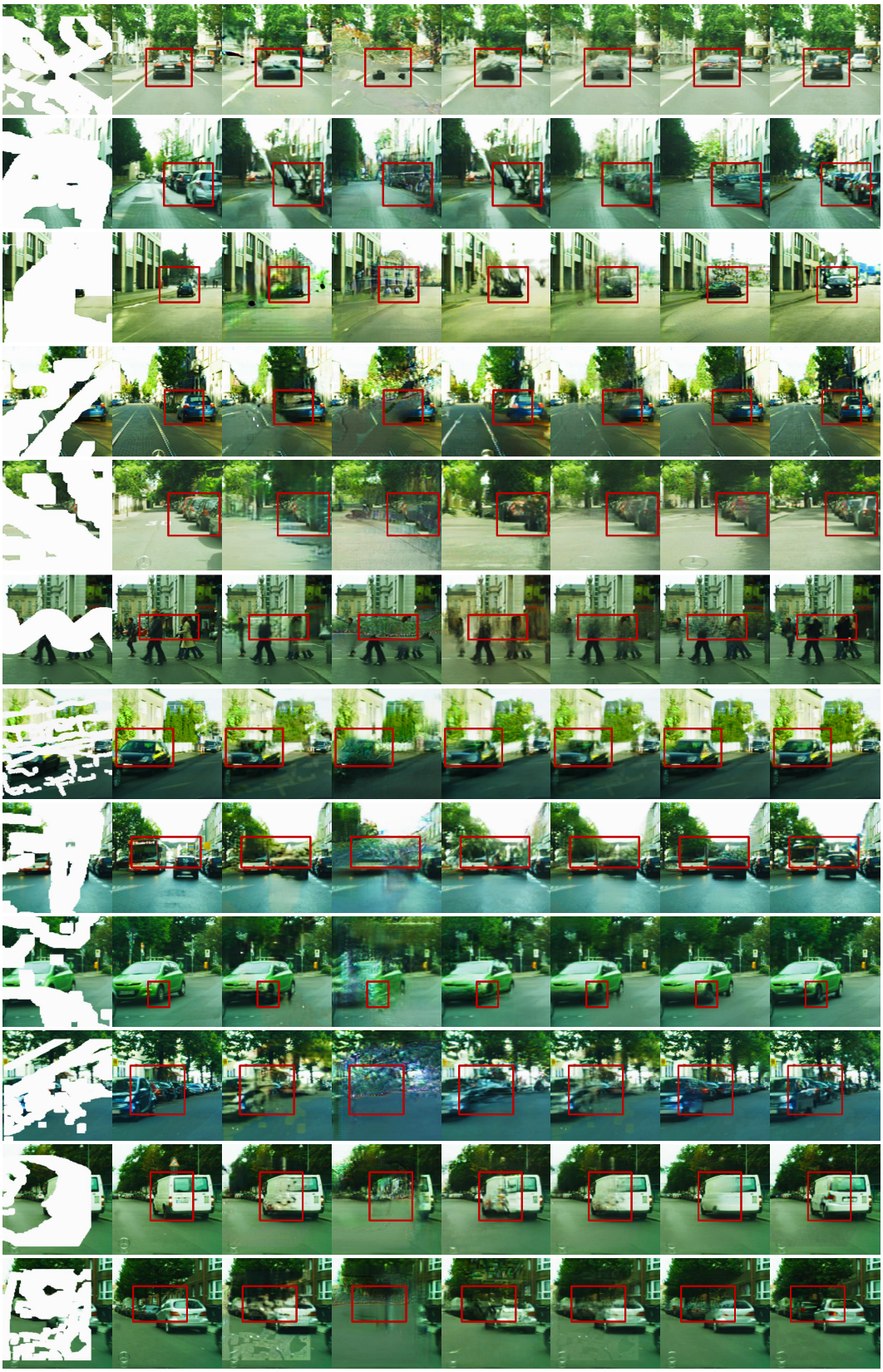

Figure 9: Visual results of Gated [2], PEN [5], SPG [6], SWAP [7], SPL [8] and CICM on the test set of Cityscapes.

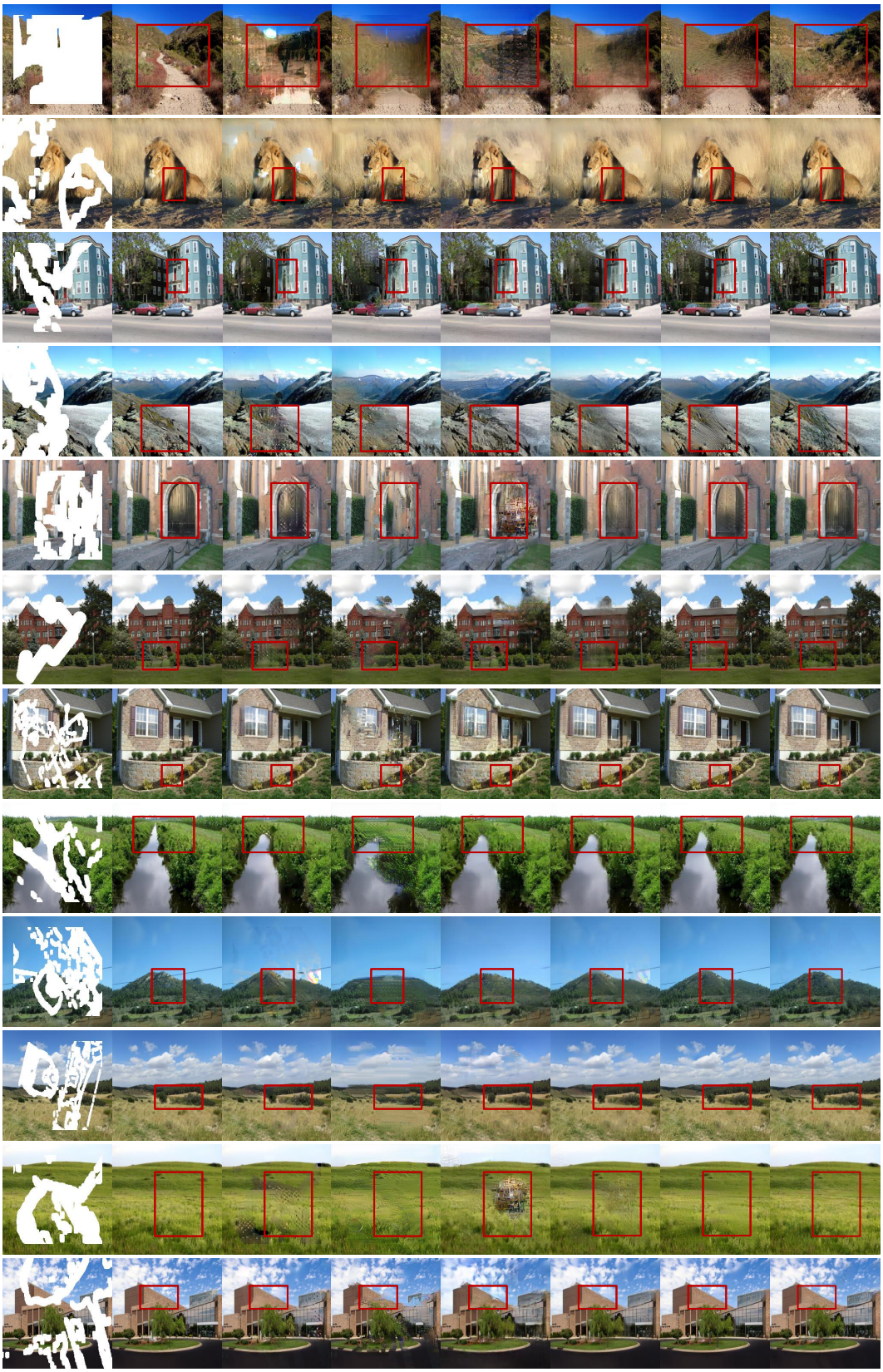

Figure 10: Visual results of Gated [2], PEN [5], SPG [6], SWAP [7], SPL [8] and CICM on the test set of Outdoor Scenes.

3 Limitation

3.1 Failure Cases

Some failure cases are shown in Figure 11 for better understanding the limitation of our method. In these cases, the input images have large scopes of the corrupted regions (see (a) and (b)). The input images provide little information for the context augmentation, disallowing the context augmentation to reliably find the relevant cross-image features in CICM, consequently offering less useful context for recovering the corrupted regions.

In some of these failure cases, the input images contains the visual information, which shows a large discrepancy with the information learned and stored in CICM. For example, the faces in Figure 11(c–d) are observed from the angles that are rarely seen in the training data. Though CICM contains the cross-image features produced by the context generalization, these challenging cases still leads to unsatisfactory results. Thus, the generalization power of CICM still need to be improved.

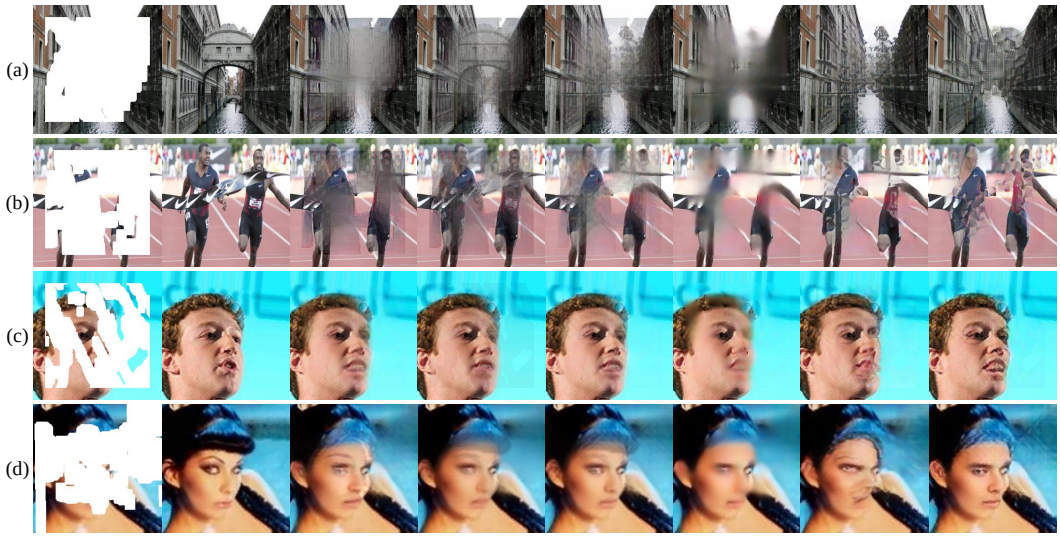

Figure 11: The visual results failure cases on the test set of Places2 and CelebA.

3.2 Memory Increase

In Table 4 (also see Table 3 of the main paper), we have justify the generalization power of CICM, which consistently improves the performances of different inpainting networks. It should be noted that CICM requires more memory budget for storing the cross-image features. In Table 5, we compare the network parameters (M), GPU memory (GB), and FLOPs (G) of the inpainting networks with and without CICM, for considering the trade-off between the inpainting performance and computational efficiency.

3.3 Evaluation of CICM in Cross-Model and -Dataset Scenarios

Note that CICM can be added to different inpainting networks. Here, we evaluate the performance of CICM, which is trained along with an inpainting networks and applied to another network. We report the results in Table 6. Here, we evaluate the inpainting performance on Place2, where the corrupted ratio is set to 20-40%.

We train the baseline UNet and the recent inpainting method MISF [12], which are equipped with CICMs respectively. Their performances are reported in the row "w/o Cross Model". Then, we exchange CICMs between UNet and MISF, where each of these CICMs are directly used for inpainting without further fine-tuning. The performances of UNet and MISF with the exchanged CICMs are reported in the row "w/ Cross Model". We find that the exchanged CICMs slightly degrade the performances of UNet and MISF. It may be because the cross-image features in the exchanged CICMs mismatch the regional features extracted by UNet and MISF. Yet, the exchanged CICMs yield better performances than the networks without CICM (see the row "w/o CICM").

Places2 Dataset															
Methods	PSNR ↑			SSIM ↑			L1 ↓			LPIPS ↓			FID ↓		
	0-20%	20-40%	40-60%	0-20%	20-40%	40-60%	0-20%	20-40%	40-60%	0-20%	20-40%	40-60%	0-20%	20-40%	40-60%
UNet	28.637	20.944	17.022	0.9141	0.7885	0.5746	1.137	3.606	7.269	0.0850	0.2162	0.3838	18.37	58.22	112.7
UNet-CICM	**29.214**	**21.728**	**18.811**	**0.9205**	**0.8047**	**0.6258**	**1.079**	**3.478**	**6.375**	**0.0829**	**0.2045**	**0.3284**	**17.21**	**45.17**	**78.49**
RFR [10]	28.891	21.278	17.648	0.9167	0.7893	0.5953	1.128	3.532	6.916	0.0873	0.2267	0.3723	17.83	51.29	95.72
RFR-CICM	**29.411**	**22.146**	**19.313**	**0.9210**	**0.8134**	**0.6311**	**1.065**	**3.337**	**6.211**	**0.0834**	**0.2088**	**0.3174**	**16.69**	**40.23**	**64.17**
JPG [11]	30.023	22.561	18.045	0.9362	0.8267	0.6762	0.902	2.671	5.725	0.0883	0.2417	0.3521	16.78	39.21	78.77
JPG-CICM	**30.457**	**23.716**	**20.016**	**0.9417**	**0.8325**	**0.7022**	**0.868**	**2.516**	**5.073**	**0.0835**	**0.2174**	**0.3093**	**16.02**	**34.88**	**58.19**
MISF [12]	31.044	23.799	19.314	0.9443	0.8312	0.6736	0.741	2.520	5.311	0.0537	0.1721	0.2821	16.39	35.31	62.67
MISF-CICM	**31.516**	**24.858**	**21.267**	**0.9491**	**0.8405**	**0.7027**	**0.712**	**2.317**	**4.872**	**0.0501**	**0.1498**	**0.2389**	**14.76**	**29.12**	**48.21**
CelebA Dataset															
Methods	PSNR ↑			SSIM ↑			L1 ↓			LPIPS ↓			FID ↓		
	0-20%	20-40%	40-60%	0-20%	20-40%	40-60%	0-20%	20-40%	40-60%	0-20%	20-40%	40-60%	0-20%	20-40%	40-60%
UNet	33.133	24.573	19.522	0.9577	0.8621	0.7234	0.533	1.882	4.623	0.0432	0.1282	0.2476	10.74	40.83	75.39
UNet-CICM	**33.388**	**25.384**	**21.673**	**0.9610**	**0.8788**	**0.7689**	**0.518**	**1.820**	**4.127**	**0.0419**	**0.1214**	**0.2238**	**8.493**	**35.47**	**63.22**
RFR [10]	33.327	25.224	20.133	0.9571	0.8722	0.7323	0.538	1.872	4.638	0.0437	0.1257	0.2421	9.362	33.28	67.31
RFR-CICM	**33.636**	**26.056**	**21.517**	**0.9601**	**0.8793**	**0.7654**	**0.515**	**1.784**	**4.164**	**0.0408**	**0.1166**	**0.2287**	**7.134**	**31.78**	**56.98**
JPG [11]	33.925	26.338	20.548	0.9573	0.8826	0.7428	0.527	1.692	4.411	0.0427	0.1307	0.2559	8.273	32.02	61.32
JPG-CICM	**34.262**	**27.027**	**22.393**	**0.9619**	**0.8902**	**0.7681**	**0.504**	**1.646**	**3.817**	**0.0401**	**0.1186**	**0.2265**	**6.374**	**29.26**	**53.87**
MISF [12]	34.302	26.387	21.289	0.9629	0.8903	0.7585	0.501	1.572	3.922	0.0336	0.0981	0.2137	6.836	30.11	55.75
MISF-CICM	**34.695**	**27.854**	**23.338**	**0.9683**	**0.9012**	**0.7782**	**0.489**	**1.502**	**3.311**	**0.0317**	**0.0925**	**0.1921**	**5.023**	**27.99**	**47.12**

Table 4: The results of combining CICM with different inpainting networks (i.e., RFR [10], JPG [11], and MISF [12]) on the test sets of Places2 and CelebA.

Methods	Parameters (M)	Memory (GB)	FLOPs (G)	Methods	Parameters (M)	Memory (GB)	FLOPs (G)
UNet	10.42	11.37	10.02	JPG	42.57	39.22	31.79
UNet-CICM	**11.21**	**13.48**	**11.75**	**JPG-CICM**	**44.21**	**42.27**	**33.51**
RFR	19.58	24.98	27.72	MISF	37.21	36.74	15.26
RFR-CICM	**20.33**	**27.33**	**29.11**	**MISF-CICM**	**38.43**	**38.15**	**17.20**

Table 5: Comparison of the network parameters (M), GPU memory (GB), and FLOPs (G) of the inpainting networks with and without CICM.

	PSNR ↑	SSIM ↑	L1 ↓	LPIPS ↓	FID ↓	PSNR ↑	SSIM ↑	L1 ↓	LPIPS ↓	FID ↓
w/o CICM	UNet					MISF				
	20.944	0.7885	3.606	0.2162	57.38	23.799	0.8312	2.522	0.1721	34.72
w/o Cross Model	UNet-CICM					MISF-CICM				
	21.728	**0.8047**	**3.478**	**0.2045**	**45.17**	**24.858**	**0.8405**	**2.317**	**0.1498**	**29.12**
w/ Cross Model	UNet-CICM (MISF)					MISF-CICM (UNet)				
	21.373	0.8001	3.554	0.2127	48.27	24.235	0.8335	2.422	0.1574	32.35

Table 6: The results of the methods replacing the CICMs of UNet-CICM and MISF-CICM on the test sets of Places2.

In Table 7, we investigate the possibility of exchanging CICMs that are trained on different datasets. Here, we train two separate UNets on Places2 and CelebA. Each UNet is associated with CICM.

	Places2					CelebA				
	PSNR ↑	SSIM ↑	L1 ↓	LPIPS ↓	FID ↓	PSNR ↑	SSIM ↑	L1 ↓	LPIPS ↓	FID ↓
w/o CICM	20.944	0.7885	3.606	0.2162	57.38	24.573	0.8621	1.882	0.1282	40.27
w/o Cross Dataset	**21.728**	**0.8047**	**3.478**	**0.2045**	**45.17**	**25.384**	**0.8788**	**1.820**	**0.1214**	**35.47**
w/ Cross Dataset	19.274	0.7672	3.936	0.2237	75.32	23.477	0.8489	2.024	0.1473	67.21

Table 7: The results of the methods replacing the CICMs of two UNet-CICM trained on Places and CelebA respectively.

After the network training, we exchange CICMs of the two UNets, which are evaluated on the test sets of Places2 and CelebA respectively (see the row "w/ Cross Dataset"). We find that the exchanged CICMs drastically degrade the performances, compared to the inpainting networks without the exchanged CICMs (see the row "w/o Cross Dataset") or even without CICM (see the row "w/o CICM"). This may because in Places2 and CelebA, the images contains scene and face information, respectively, showing a weak correlation. Thus, the cross-image features in the exchanged CICMs likely mislead the context augmentation.

4 Code Segment

Our code will be available at: https://github.com/fengtl/CICM.

References

[1] Guilin Liu, Fitsum A Reda, Kevin J Shih, Ting-Chun Wang, Andrew Tao, and Bryan Catanzaro. Image inpainting for irregular holes using partial convolutions. In *European Conference on Computer Vision*, pages 85–100, 2018.

[2] Jiahui Yu, Zhe Lin, Jimei Yang, Xiaohui Shen, Xin Lu, and Thomas S Huang. Free-form image inpainting with gated convolution. In *IEEE/CVF International Conference on Computer Vision*, pages 4471–4480, 2019.

[3] Yurui Ren, Xiaoming Yu, Ruonan Zhang, Thomas H Li, Shan Liu, and Ge Li. Structureflow: Image inpainting via structure-aware appearance flow. In *IEEE/CVF International Conference on Computer Vision*, pages 181–190, 2019.

[4] Sungwon Park, Sungwon Han, Sundong Kim, Danu Kim, Sungkyu Park, Seunghoon Hong, and Meeyoung Cha. Improving unsupervised image clustering with robust learning. In *IEEE/CVF Conference on Computer Vision and Pattern Recognition*, pages 12278–12287, 2021.

[5] Yanhong Zeng, Jianlong Fu, Hongyang Chao, and Baining Guo. Learning pyramid-context encoder network for high-quality image inpainting. In *IEEE/CVF Conference on Computer Vision and Pattern Recognition*, pages 1486–1494, 2019.

[6] Yuhang Song, Chao Yang, Yeji Shen, Peng Wang, Qin Huang, and C-C Jay Kuo. Spg-net: Segmentation prediction and guidance network for image inpainting. In *British Machine Vision Conference*, 2018.

[7] Liang Liao, Jing Xiao, Zheng Wang, Chia-Wen Lin, and Shin'ichi Satoh. Image inpainting guided by coherence priors of semantics and textures. In *IEEE/CVF Conference on Computer Vision and Pattern Recognition*, pages 6539–6548, 2021.

[8] Wendong Zhang, Junwei Zhu, Ying Tai, Yunbo Wang, Wenqing Chu, Bingbing Ni, Chengjie Wang, and Xiaokang Yang. Context-aware image inpainting with learned semantic priors. In *International Joint Conference on Artificial Intelligence*, 2021.

[9] Laurens Van der Maaten and Geoffrey Hinton. Visualizing data using t-sne. *Journal of Machine Learning Research*, 9(11), 2008.

[10] Jingyuan Li, Ning Wang, Lefei Zhang, Bo Du, and Dacheng Tao. Recurrent feature reasoning for image inpainting. In *IEEE/CVF Conference on Computer Vision and Pattern Recognition*, pages 7760–7768, 2020.

[11] Qing Guo, Xiaoguang Li, Felix Juefei-Xu, Hongkai Yu, Yang Liu, and Song Wang. Jpgnet: Joint predictive filtering and generative network for image inpainting. In *ACM International Conference on Multimedia*, pages 386–394, 2021.

[12] Xiaoguang Li, Qing Guo, Di Lin, Ping Li, Wei Feng, and Song Wang. Misf: Multi-level interactive siamese filtering for high-fidelity image inpainting. In *IEEE/CVF Conference on Computer Vision and Pattern Recognition*, pages 1869–1878, 2022.

[13] Rui Xu, Minghao Guo, Jiaqi Wang, Xiaoxiao Li, Bolei Zhou, and Chen Change Loy. Texture memory-augmented deep patch-based image inpainting. *IEEE Transactions on Image Processing*, 30:9112–9124, 2021.

[14] Xin Feng, Wenjie Pei, Fengjun Li, Fanglin Chen, David Zhang, and Guangming Lu. Generative memory-guided semantic reasoning model for image inpainting. *arXiv preprint arXiv:2110.00261*, 2021.